Journal Pre-proof

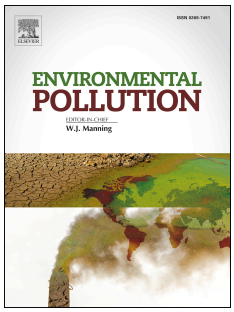

Plastics, (bio)polymers and their apparent biogeochemical cycle: an infrared spectroscopy study on foraminifera

Giovanni Birarda, Carla Buosi, Francesca Caridi, Maria Antonietta Casu, Giovanni De Giudici, Letizia Di Bella, Daniela Medas, Carlo Meneghini, Martina Pierdomenico, Anna Sabbatini, Artur Surowka, Lisa Vaccari

PII: S0269-7491(21)00494-2

DOI: https://doi.org/10.1016/j.envpol.2021.116912

Reference: ENPO 116912

To appear in: *Environmental Pollution*

Received Date: 15 December 2020

Revised Date: 20 February 2021

Accepted Date: 4 March 2021

Please cite this article as: Birarda, G., Buosi, C., Caridi, F., Casu, M.A., De Giudici, G., Di Bella, L., Medas, D., Meneghini, C., Pierdomenico, M., Sabbatini, A., Surowka, A., Vaccari, L., Plastics, (bio)polymers and their apparent biogeochemical cycle: an infrared spectroscopy study on foraminifera, *Environmental Pollution*, https://doi.org/10.1016/j.envpol.2021.116912.

Author statement

In this work, FC and AS cultured foraminifera in AQ University laboratory and provided foraminifera to CB and DM that cultured foraminifera in CAG University. LDB and MP provided EPB41 samples. MAC provided microtome cuts. AS, GB and LV conducted FTIR data collection and analysis. GDG, CM and DM coordinated CERIC-ERIC research activities. All the authors equally contributed to the experiment conception and writing the paper.

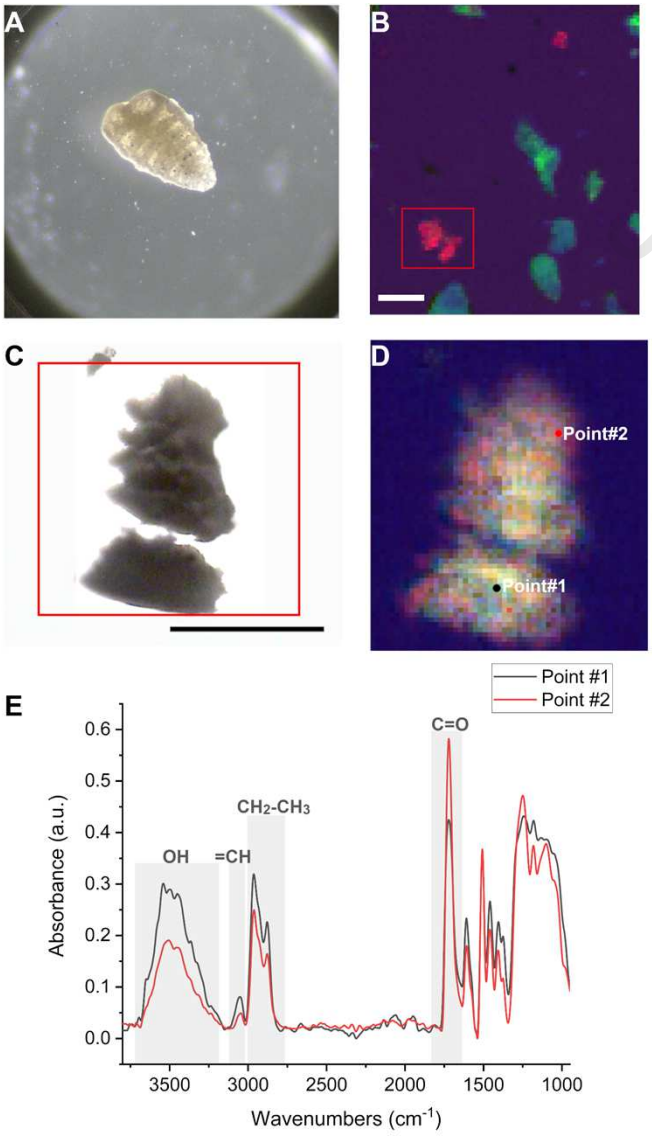

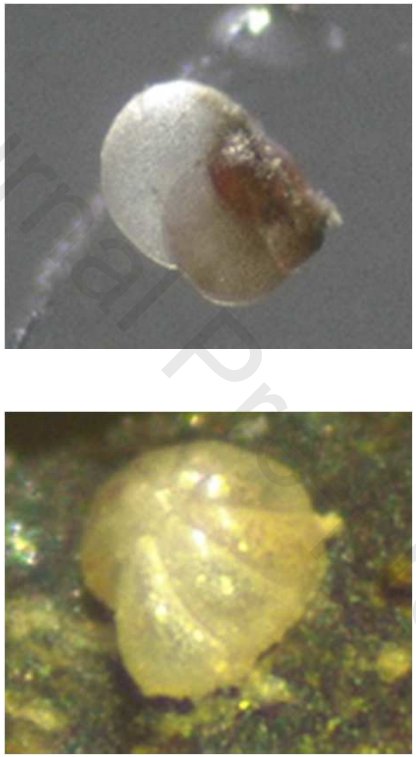

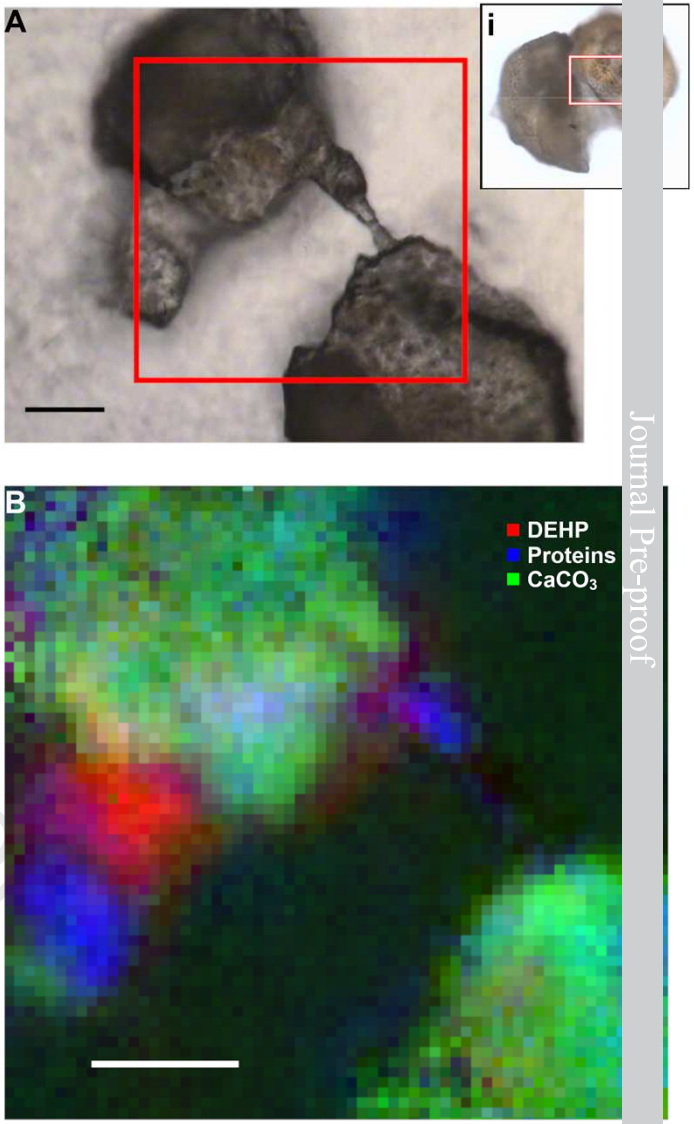

Plastics, (bio)polymers and their apparent biogeochemical cycle: an infrared spectroscopy study on foraminifera

Giovanni Birarda[a], Carla Buosi[b], Francesca Caridi[c], Maria Antonietta Casu[d], Giovanni De Giudici[b]*, Letizia Di Bella[e], Daniela Medas[b], Carlo Meneghini[f], Martina Pierdomenico[g], Anna Sabbatini[c], Artur Surowka[a,h], Lisa Vaccari[a].

[a] Elettra-Sincrotrone Trieste S.C.p.A., SS 14, km 163,5, Basovizza, Trieste, TS 34149, Italy

[b] Department of Chemical and Geological Sciences – University of Cagliari, Cittadella Universitaria S.S. 554 bivio per Sestu, 09042 Monserrato (CA), Italy

[c] Dipartimento di Scienze della Vita e dell'Ambiente, Facoltà di Scienze, Università Politecnica delle Marche Via Brecce Bianche, 60131 Ancona, Italy

[d] National Research Council of Italy, Institute of Translational Pharmacology, UOS of Cagliari, Scientific and Technological Park of Sardinia POLARIS, Pula, Italy

[e]Department of Earth Science, Rome University "Sapienza", P.le A. Moro 5, 00185 Rome, Italy

[f]University of Rome Tre, Department of Sciences, Viale G. Marconi 446, 00146 Roma, Italy

[g]Istituto per lo studio degli impatti Antropici e Sostenibilità in ambiente marino (CNR-IAS), Roma, Via della Vasca Navale 79, 00146, Rome, Italy

[h] AGH University of Science and Technology, Faculty of Physics and Applied Computer Science, al. Mickiewicza 30, 30-059 Kraków, Poland

*corresponding author: gbgiudic@unica.it

Abstract.

To understand the fate of plastic in oceans and the interaction with marine organisms, we investigated the incorporation of (bio)polymers and microplastics in selected benthic foraminiferal species by applying FTIR (Fourier Transform Infrared) microscopy. This experimental methodology has been applied to cultured benthic foraminifera *Rosalina globularis*, and to *in situ* foraminifera collected in a plastic remain found buried into superficial sediment in the Mediterranean seafloor, *Rosalina bradyi*, *Textularia bocki* and *Cibicidoides lobatulus*. *In vitro* foraminifera were treated with bis-(2-ethylhexyl) phthalate (DEHP) molecule to explore its internalization in the cytoplasm. Benthic foraminifera are marine microbial eukaryotes, sediment-dwelling, commonly short-lived and with reproductive cycles which play a central role in global biogeochemical cycles of inorganic and organic compounds. Despite the recent advances and investigations into the occurrence, distribution, and abundance of plastics, including microplastics, in marine environments, there remain relevant knowledge gaps, particularly on their effects on the benthic protists. No study, to our knowledge, has documented the molecular scale effect of plastics on foraminifera.

Our analyses revealed three possible ways through which plastic-related molecules and plastic debris can enter a biogeochemical cycle and may affect the ecosystems: 1) foraminifera *in situ* can grow on plastic remains, namely *C. lobatulus*, *R. bradyi* and *T. bocki*, showing signals of oxidative stress and protein aggregation in comparison with *R. globularis* cultured in negative control; 2) DEHP can be incorporated in the cytoplasm of calcareous foraminifera, as observed in *R. globularis*; 3) microplastic debris, identified as epoxy resin, can be found in the cytoplasm and the agglutinated shell of *T. bocki*.

We hypothesize that plastic waste and their associated additives may produce modifications related to the biomineralization process in foraminifera. This effect would be added to those induced by ocean acidification with negative consequences on the foraminiferal biogenic C storage capacity.

1. Introduction

Plastics are emerging pollutant at the global scale that, with ca. 5 billion tons of waste dispersed in the environment, is affecting the oceans and the trophic chain (Geyer et al., 2017). It has been recently estimated that 5−8 million tons of plastic move from land to oceans every year (Jambeck et al., 2015) also reaching the deep ocean floor (Peeken et al., 2018). Plastics have then to be regarded as an analogue of sedimentary materials, as they undergo through their biogeochemical cycle characterized by a grain size comminution associated to some change in structural properties (Cau et al., 2020; and references therein). Microplastics are generally referred to the size smaller than 5 mm (Picó and Barceló, 2019, and references therein) and can be further classified into subcategories depending on their dimension. The amount of microplastics attaining the oceans varies in the range of 0.13 and 0.28 million tons per year (IUCN, https://www.iucn.org/theme/marine-and-polar/our-work/close-plastic-tap-programme/reports). In turn, primary microplastics can become secondary microplastics due to physical and mechanical processes occurring in the oceans. Environmental microplastic pollution is recognized to have long persistence ranging from decades to hundreds of years (Auta et al., 2017 and references therein; Enders et al., 2019; Shim and Thompson, 2015; Vandermeersch et al., 2015). Despite undoubtedly long-term harmful impact to microbiota, the fate of microplastics, chemicals and synthetic molecules incorporated into both the cytoplasm and skeletons of marine micro-organisms is still poorly understood (Baztan et al., 2018; de Sá et al., 2018).

A growing body of literature investigates ecotoxicological effects of plastics. Redondo-Hasselerharm et al. (2018) found that plastic pollutants endanger macroinvertebrate at high concentration, however, even if the risks of environmentally realistic concentrations of microplastics may be low, they still may affect the biodiversity and the functioning of aquatic communities which after all also depend on the sensitive species. Microplastics can interact with the plankton thus entering the food web (Pazos et al., 2018), and this likely results in bis-(2-ethylhexyl) phthalate (DEHP) accumulation across the food web (Fossi et al., 2012).

DEHP is a moderately water-soluble synthetic molecule (Gibbons and Alexander, 1989; Luo et al., 2018), industrially produced, and used in plasticizers, industrial solvents and lubricants, additives in the textile industry, in pesticide formulations, and in bodycare products such as deodorants, perfumes, or hairsprays (Graham, 1973; Koo and Lee, 2004; Stanley et al., 2003). While the DEHP molecule does not exist in nature, having only an industrial origin, several phthalic diesters occur as natural products (Hoang et al., 2008; Ljungvall et al., 2008; Roy et al., 2006), making it suitable for strong bio-interactions in the ecosystem. The presence of carbonyl groups suggests that reactivity of DEHP may show some analogies with other organic and natural molecules, such as amino acids, lipids and polysaccharides, commonly associated to cyanobacterial activity (Singh et al., 2002), specifically to monostearin (Sanna et al., 2015) or succinic acid and fumaric acid, both components of the citric acid cycle. DEHP can be incorporated in hundreds of ppm in carbonate minerals providing us a suitable proxy for mineral-biosphere interactions (Sanna et al., 2015). Moreover, DEHP contains ester groups that are also present in molecular components of foraminifera, which causes that the DEHP may reveal some affinity to them even though its overall chemical scaffold is radically different (see Sanna et al., 2015 and references therein).

The open questions are how much the fate of plastics is affected by biological activities, where grain size comminution and interaction with tissues and biological fluids occur. To shed light on these questions, the different compartments of the biogeochemical cycle of plastics must be investigated.

In this work, to explore the fate of plastic debris in marine habitats we focus on benthic foraminifera. These unicellular organisms, ubiquitous in the marine realm, colonize both the water column and the sediment. In the global carbonate budget, foraminifera are one of the major calcifiers contributing to the carbonate production (Kawahata et al., 2019). It has been estimated that all benthic foraminifera annually produce 200 million tons of calcium carbonate worldwide (Langer, 2008). Larger symbiont-bearing foraminifera play a prominent role as carbonate producers in modern tropical environments (reef and shelf areas), with an estimated production of at least 130 million tons of $CaCO_3$ per year. This amount corresponds to approximately 2.5% of the $CaCO_3$ of the annual present-day carbonate

production in all oceans (Langer, 2008). These data highlight the importance of foraminifera within the $CaCO_3$ budget of the marine realm. Because of foraminifera are sensitive to changes in the oceanic environment and their calcareous test preserve a record of ocean chemical variations, they can be considered as useful indicators of past climate and environmental changes (Boyle and Keigwin, 1985; Curry et al., 1998; Langer, 2008).

Foraminifera can be used also to define the present Ecological Quality Status (EcoQS) (e.g., Barras et al., 2014; Bouchet et al., 2018; Damak et al., 2019; Fossile et al., 2021) and to provide time series back to reference conditions (e.g., Alve et al., 2009; Dolven et al., 2013). Their distribution and composition are influenced by several environmental factors including temperature, salinity, organic matter inputs, oxygen, sediment grain size and composition (Celia Magno et al., 2012; Murray, 2006; Sen Gupta, 1999). Based on such features, foraminifera are widely used as bioindicators of different impacts in coastal environments: aquaculture, oil spills, harmful metals and urban sewage (e.g. Bouchet et al., 2020; Parsaian et al., 2018; Vénec-Peyré et al., 2020), even though it is still controversial the distinction between natural and anthropogenic stress (Armynot du Châtelet and Debenay, 2010).

In a fairly large body of literature, foraminifera are investigated by *in situ* and/or *in vitro* experiments to dissect their response to changes in one or more chemical-physical parameters under controlled conditions, either at the level of the whole fauna (in micro- or mesocosms) or of one or a few selected species (in culture). The results obtained in the laboratory could represent a model, albeit simplified, of ecosystem functioning, and can be tested *in situ*.

It is noteworthy that accumulation of microplastics in foraminifera may be an entry of such particles into the marine benthic food webs but there is a severe lack of knowledge on whether and how this issue may affect benthic foraminifera. Grefstad (2019) fed several benthic calcareous foraminiferal species during a four-week experiment using fluorescent polystyrene microspheres. The author showed that there are differences in the accumulation of microplastics in benthic foraminiferal species driven by their food preferences and test composition. Langlet et al. (2020) monitored the short-term effect of polypropylene (PP) leachates at both environmentally realistic and chronic concentrations on the locomotion and metabolism of benthic calcareous foraminifera. They found that PP leachates have no lethal effects on this species activity. For these reasons, they suggest that benthic foraminifera may be more resistant than other marine invertebrates (i.e., mollusks, fishes) to plasticizers pollutants. Studies cited above tested the foraminiferal ability to accumulate plastics in the cell and the resistance to their potentially toxic effects. But no study, to our knowledge, has documented the effect of DEHP on foraminifera.

Fourier Transform Infrared spectroscopy (FTIR) is a well-established analytical technique that provides chemical information about the inspected samples (Silverstein et al., 2005). About 30 years ago, FTIR spectroscopy was coupled with microscopes, becoming FTIR spectromicroscopy (µ-FTIR), allowing for a spatially resolved chemical characterization of materials ranging from polymers (Kellner et al., 1986; Kellner and Weigel, 1988) to biological samples like bacteria and eukaryotic cells (Legal et al., 1991; Wetzel and LeVine, 1999). Moreover, it was possible to push the resolution to the diffraction limit by using high brilliant sources like Synchrotrons (Holman et al., 2000; Jamin et al., 1988). Nowadays µ-FTIR is commonly used in manifold scientific fields, like chemistry, materials sciences, pharmaceutics, physics and in particular in biology, where it is routinely employed to probe cellular statuses (Doherty et al., 2017) or diagnose healthy and diseased tissues (Movasaghi et al., 2008).

In this work, we considered three foraminiferal species from the Mediterranean Sea and one cultured in laboratory to be representative of the main taxonomic groups having different types of building test: the calcareous species which precipitate $CaCO_3$ to build their case and the agglutinated taxon that allocates particles of different type and size held together by a biochemical or Ca-carbonate cement (Sen Gupta, 1999).

Therefore, the present study aimed to evaluate the effects of exposure of microplastics in foraminiferal specimens (*Cibicidoides lobatulus*, *Rosalina bradyi* and *Textularia bocki*) grown attached to plastic debris and collected into the sandy-silt sediment of the Mediterranean seafloor. Also, this research will focus then on the investigation of the DEHP molecule incorporation in the cytoplasm and calcareous test of *R. globularis* grown in critical exposure of this plastic additive.

2. Material and Methods

2.1. Samples from laboratory cultures

Culturing foraminifera was necessary to obtain and to maintain specimens for experimental purposes. Specimens of *R. globularis*, used in this study, were grown in monospecific cultures set up at the Laboratory of Paleoecology of the DISVA (UNIVPM). For foraminiferal culture maintenance we followed Caridi et al. (2020).

For the experiment, we selected foraminiferal tests in a size range from 90 to 150 µm in order to have adult specimens and not juvenile forms, which could bias the taxonomic identification. Then, we observed them under the stereomicroscope NIKON SMZ-U to check their vitality. In particular, vitality was assessed by the presence of sediment particles close to the aperture and/or yellow/brown colour; these specimens were further observed under the optical microscopy Nikon Eclipse E 600 POL with phase contrast, in order to further detect pseudopodial activity.

One foraminiferal taxon (*R. globularis*) was picked from culture using a fine brush. Alive specimens were selected using phase contrast optical microscopy (please see above), and then each specimen was randomly transferred in three different series (replicates) of sterile plastic jars. In particular, in total n=4 plastic jars were prepared for the experiment: n=3 replicates each containing n=5 specimens of *R. globularis*, including controls (n=1 jar) for a total of n=20 specimens, in this work we show results only from some of the specimens.

Acute concentration of DEHP was tested, formally 500 mg/L neat liquid added to solution resulting in ca. 0.3 mg/L dissolved (Gibbons and Alexander, 1989), plus one control concentration (nominally 0 mg/L). 20 µl pure neat DEHP aliquots were added to 40 mL of filtered seawater and kept in a room temperature for 7 weeks. The cultures were incubated at 15°C, following the day-night cycle and fed with few drops of freeze-killed *Isochrysis galbana* every two weeks. Conditions of pH of 8.0±0.1 and salinity of 35 were kept stable for the duration of the experiment, with weekly replacement of experimental solution of DEHP. Salinity adjustments were performed by adding deionized water.

2.2. Samples from Mediterranean seabed

Thirteen grabs (30 L Van Veen grab) were collected during the EPICA cruise carried out in the Southern Tyrrhenian sea, along the NE Sicilian continental margin (Patti basin). The expedition took place from December 16, 2015 to January 3, 2016 on board of the R/V Minerva Uno of the Italian National Research Council (CNR). At station EPB41, located at 82 m depth within the thalweg of small gullies in front of the Mazzarrà River mouth (Casalbore et al., 2017), a black plastic bag (about 30x30cm probably constituted of polyethylene material) was found buried into sandy silt sediment, completely colonized by meio- and macrofaunal communities (bivalves, hydrozoa, gorgonians, polychaetes, ascidians, foraminifera, briozoans). The plastic bag was cut into about 30 fragments (about 5x5cm) and analyzed by means of stereomicroscope to pick foraminifera living on the plastic surface. In this study, foraminiferal specimens belonging to *R. bradyi*, *C. lobatulus* and *T. bocki*, were considered. Only the well-preserved tests, recorded in attached life position on the plastic remain, were carefully detached from the plastic surface. Classification of the taxa was carried out on the literature guidelines (Cimerman and Langer, 1991; Sgarrella and Moncharmont-Zei, 1993). Taxonomical identification was based on World Register of Marine Species (WoRMS, 2020). Table 1 resumes the investigated samples. In total, we analyzed n=10 specimens for each species (*R. bradyi*, *C. lobatulus* and *T. bocki*), in total n=30 specimens. Samples investigated by FTIR analysis. Additional information on foraminifera is provided in the Appendix.

Table 1.
Foraminifera investigated in this study. Pictures from EPB41 samples were taken on samples attached on the plastic remain before washing and picking.

SAMPLE	SOURCE/COLLECTION	PICTURE	DIAMOND ANVIL CELL (DAC)	RESIN EMBEDDED THIN SECTION
Rosalina globularis	unpolluted in vitro grown (S5) – negative control		8 maps*	2 maps
Rosalina globularis	DEHP polluted in vitro grown (S9) – positive control		28 maps	
Cibicidoides lobatulus	Mediterranean EPB41 (S3)		6 maps	6 maps
Rosalina bradyi	Mediterranean EPB41 (S8)		5 maps	7 maps
Textularia bocki	Mediterranean EPB41 (S1)	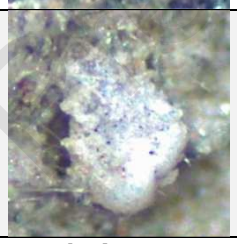	12 maps	1 map

*Each map can be 1x1 tile or be a mosaic of multiple tiles, each tile contains 4096 spectra.

2.3. FTIR

Samples were measured at SISSI beamline at Elettra Sincrotrone Trieste using a Bruker Hyperion 3000 IR-VIS microscope coupled with a Vertex 70V in vacuum interferometer. As reported in Table 1, the harvested samples were divided into two groups and underwent a different processing before being measured. In order to prepare thin sections for FTIR microscopy, foraminiferal shells were immersed in 100% resin (Epon 812) for 30 min at room temperature, followed by polymerization at 60°C for 48 h. Semi-thin sections (1 µm) were cut with a diamond knife on ultramicrotome and deposited onto CaF_2 windows. Some of the samples were picked up from solutions, deposited onto a diamond compression cell (Diamond Anvil Cell -DAC – X'press - Japan) and crushed to obtain flat pieces few microns thick and then measured by FTIR. Single foraminiferal specimens were picked up from the solution and dissected under the microscope into small fragments of shell and cellular part. The extracted parts were

placed onto the open DAC. Once the DAC was closed and the pressure was applied by tightening the screws, the samples were pulverized and thinned to allow for transmission measurements. In some cases, to maintain substantial morphology of the samples, very small fragments were imaged (see the next section).

FTIR spectra of the resin embedded sections and DAC samples were measured in transmission mode using a 15X objective and condenser and a Focal Plane Array (FPA) detector. The FPA detector has a sensitive overview area of 168×168 µm divided in 64×64 pixels, and therefore every hyperspectral image contains 4096 spectra, with the effective pixel size of 2.6×2.6 µm per pixel. To survey the sample to find any area of interest, low-resolution images of the whole samples were firstly acquired using pixel binning at 4×4 (10.5×10.5 µm per pixel) with 16 scans and at 16 cm^{-1} spectral resolution. Then, images at higher lateral and spectral resolution were collected without binning, co-adding 256 scans and at 4 cm^{-1} spectral resolution. For the samples grown in DEHP polluted environment, single point spectra were collected with a Mercury Cadmium Telluride (MCT) detector, with 50×50 aperture size and 256 scans at 4 cm^{-1}. The data were analyzed in OPUS (Bruker Optics) and by in house code written in Python 3.5 using its routine numpy, scipy and matplotlib modules (Harris et al., 2020; Hunter, 2007).

2.4. Data processing: Fixative removal for resin-embedded samples

To remove the contribution of the embedding resin from the collected images an automated procedure was developed. First, the spectra from the thin section images were cut to the 970-1770 cm^{-1} spectral ranges, and vector-normalized (to account for differences from thickness/density). Data with weak absorbance, mainly attributed to the substrate and the resin, were rejected, by using the height of the peak height at 2560 cm^{-1} (overtone calcium carbonate) as a discriminator factor: all data with this peak value ≤0.1 were treated as “empty areas” and were eventually substituted with the zero vector of the respective size (to make them easier for identification in the dataset). Such images were finally subjected to simple image processing by the median filtration and closing transformations to remove isolated pixels from the image.

Within the pre-filtered data, it was critical to discriminate the areas of the samples that belong to the shell and of the cellular compartments, minimizing the contribution of the embedding medium. As a matter of fact, the spectra of resin have an intense signal at 1735 cm^{-1}, whereas the pixels belonging to the foraminifera have a relatively intense band at 1033 cm^{-1}. Therefore, by computing the ratio of the signals at 1735 cm^{-1}/1033 cm^{-1}, it is possible to discriminate the two components. In the end, the pixels characterized by this ratio between 0.1-1 yielded clean foraminifera spectra that are presented and discussed in the next sections. Additional information is provided in the Appendix.

3. Results

3.1. Direct incorporation and oxidation of microplastics in Textularia bocki

Among the foraminifera found on the plastic bag from EPB41 grab, a specimen of *Textularia bocki*, an epiphytic foraminifer that build its shell by agglutinating sediment grains, was extracted from the flask and inspected under the optical microscope (Fig. 1 A). Right upon dissecting it, a white particle emerged from inside the shell (Fig. 1 B-C-D). From the dissection process and the shape of the particle, that is 100×150 microns in size, it could be speculated that the organism and its shell grew around the particle.

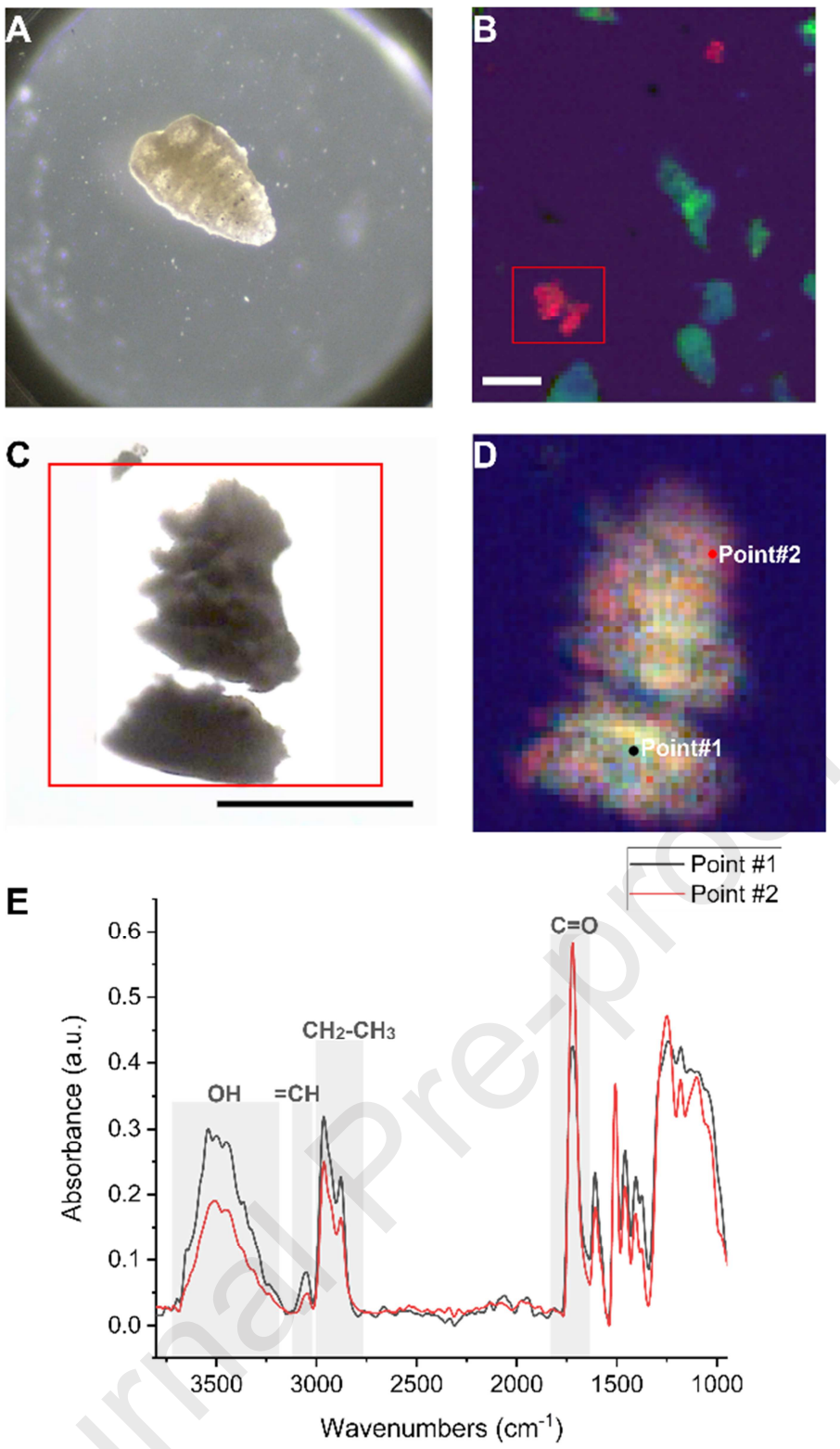

Fig. 1. A) optical image of intact *T. bocki* specimen (S1, EPB41 II) deposited onto the diamond anvil cell. B) RGB FTIR image of *T. bocki* (S1, EPB41 II) sectioned by inside the diamond anvil cell: C=O ester band at ~ 1720 cm^{-1} (red), the calcium carbonate overtone 2700-2500 cm^{-1} (green), the blue represents the amide II from protein material. C) Optical image of the debris found inside the sample. D) false color RGB map obtained integrating the C=O ester band at ~ 1720 cm^{-1} (red), the CH_2-CH_3 stretching 3000-2800 cm^{-1} (green), the blue is the C=C-H stretching 3100-3000 cm^{-1}. E) Average spectrum extracted from the FTIR image in panel D. Scale bars 100 microns.

In Fig. 1B, a heat map obtained by integrating the signals of interest for the shell/particle is presented in false color. For doing so the following bands were integrated: calcium carbonate (green), a strong peak

from the released non-foraminiferal-material at 1723 cm^{-1} (red), and the signal from amide II (1580-1480 cm^{-1}) (blue). From this image composite, it is possible to see that the red particle has a chemical composition completely different in respect of the shell material. Moreover, there are even more red particles with similar chemical composition, to be found within the sample's debris.

More detailed spectroscopic analysis of this particle is shown in Fig.s 1D-E. From these data, we can see that the particle has an overall homogenous composition, with some red areas at the edges. i.e. oxidized, but better preserved in the center, with more C=C, that are usually prone to oxidize.

By comparing the particle spectra, presented in Fig. 1E, with those in a database, the best match was an epoxy resin (Wiley, 2020). Since this organism was harvested in the sea, it is likely that the englobed particle was incorporated in the foraminifera within the shell and later became its part of this during the growth stage. To confirm this hypothesis, it is possible to bring further evidence for degradation of the polymer, which, when compared to a spectrum of a pristine epoxy resin, presents broader peaks, traces of oxidation and hydrolysis detectable by the strong C=O peak and –OH peak and local decrease of the double bonds.

By analyzing the variations of average spectra of two selected points, it is possible to see that the unknown debris is characterized by a strong variability of signal at 1723 cm^{-1} that originates from C=O, stronger at point #2 and weaker at #1 (red and black dots Fig. 1 D respectively, and spectra in Fig. 1E). Another prominent feature involved a strong signal in the CH_2- CH_3 stretching range (2800-3000 cm^{-1}, shown as green channel in Fig. 1D). From the spectra in Fig. 1E, it is possible to notice that the point #1 has a higher content of aliphatic chains in respect to #2, this correlates perfectly with in the partial oxidation of #2, and areas in the particle's image that appear "orange-red". In addition, we could also identify a variation of the intensity of the band at 3050 cm^{-1} (shown as blue channel in Fig. 1D), that could be assigned to olefin $=CH_2$ moieties.

3.2. Comparison with negative control using oriented thin sections

As a first step, we checked for differences between wild type *R. bradyi* collected from plastic sea residue, and *R. globularis* specimens, grown in clean water in the laboratory. Thin sections of foraminiferal specimens were analyzed by FTIR imaging. Embedding medium was artificially removed as described in the previous section and Supplementary material, yielding a resin free map. In this work, we show the most relevant results, concerning *R. globularis* and *R. bradyi*.

In Fig. 2A, a slice of *R. globularis*, deposited onto CaF_2 is presented. The optical image in Fig. 2A shows partial sub-axial sections of *R. globularis* where two chambers and monolamellar septa are visible. The Fig.s 2B and 2D are RGB false-color images, that were obtained by blending three infrared chemical images: the red channel represents the distribution of proteins by integrating Amide I, the green channel represents the chemical distribution of the calcium carbonate of the shell, and the blue channel shows the distribution of phosphates, either from the biochemical component of the shell and cytoplasm. A large and fast overview scan of the sample allowed the identification of the desired organic compartments on all the sections deposited on one CaF_2 slide (data not shown). In Fig. 2B, it is possible to identify the two chambers delimited by the monolamellar septum of calcium carbonate of *R. globularis* (in green in the picture); proteins and phosphates portrayed by RGB false-color image highlight the organic components and in particular the dried cytoplasm. In Fig.s 2 C-D, the same representation is used for a longitudinal section of *R. bradyi* harvested from a plastic bag from the Mediterranean. At a first glance, when compared with the map in Fig. 2 B, it seems that the organic signal from *R. bradyi* is suppressed, thus pointing to lower metabolic activity due to the interference of the plastic support. This phenomenon is even more evident in Fig. 2E, where the average spectra from the two species and their differences are shown. By analyzing the spectrum of *R. globularis*, it is possible to clearly distinguish the Amide A (3300 cm^{-1}) and Amide I (1650 cm^{-1}) peaks, which are almost undetectable in *R. bradyi*. This is more evident when analyzing the difference spectrum, which looks almost like a pure protein spectrum. We attributed this to the low amount of organic material present in the slice. As it comes to the shell composition, the calcium carbonate main peak at 1410 cm^{-1}

appears to be the same in both samples. An interesting spectral detail that can be observed for this band, it is a shoulder at 1460 cm^{-1} along to the main peak, suggesting that the shell of both may contain a mixture of crystalline and amorphous calcium carbonate.

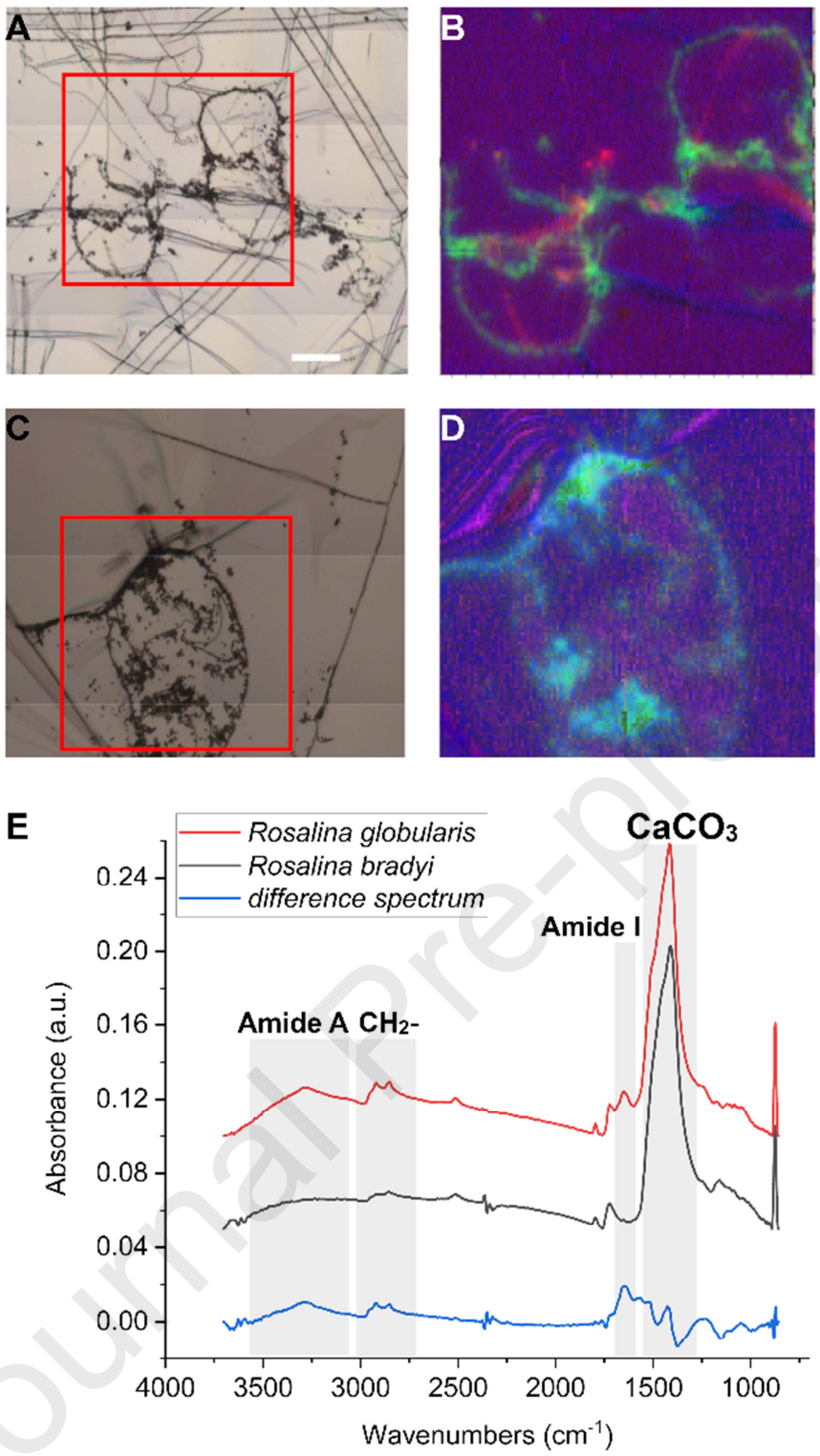

Fig. 2. A-B) optical image and RGB false-color images of *R. globularis* deposited onto CaF_2. **C-D)** optical image and FTIR imaging analysis of a longitudinal section of *R. bradyi* harvested from a plastic bag from the Mediterranean Sea (S8, EPB41). **E)** Comparison between *R. globularis* (culture, red line) and *R. bradyi* (plastic bag, black line) and difference spectrum obtained by subtracting *R. bradyi* from *R. globularis*. Scale bars= 100 microns [A,C].

3.3. Analysis of cellular stress in benthic foraminifera

The DAC measurements of *R. globularis* (sample S5), yielded more pixels with a significantly higher amount of biochemical component if compared with *R. bradyi* (S8), in accordance with what was observed in the thin sections. In Figure 3A are shown small fragments of a *R. bradyi* (S8) inside the DAC cell. The size of the particle goes from few tenths to hundreds of microns, and they are either parts of the shells or they can also contain some cellular components.

As a matter of fact, in DAC samples, the Amide I signal turned out to be strong enough to allow for a more in-depth analysis of the protein conformation through the analysis of the second derivatives. To this purpose, the amide I band is the most studied band for the determination of the conformation of proteins using FTIR (Barth, 2007) and by analyzing the sub-components of this band it is possible to determine their secondary structure. For *R. bradyi* (S8) samples we could see an increase in the high-wavenumber part of amide I, indicative of accumulating misfolded forms of proteins: beta-sheets and turns (ca. 1660-1690 cm^{-1}). In addition, the main component of amide I red-shifts towards 1642 cm^{-1}. In the foraminifera cells, a decrease in alpha-helix component and a contextual increase in beta-sheet structures are signals of cellular stress, which can lead also to apoptotic processes (Frontalini et al., 2015). Significative differences emerged for *R. globularis* specimens grown under the laboratory conditions (S5) that were found with a protein-rich cytoplasm (Fig. 3B, blue line). Specifically, it seemed to be particularly enriched in alpha-helical conformations (the band at 1654 cm^{-1}), along with a strong component at 1642 cm^{-1}, indicative of unordered forms. Considering the shell composition, as it was observed for thin sections, the calcium carbonate signal is quite similar for the two systems, whereas the low-wavenumber part (down to 1000 cm^{-1} mainly phosphates) of the FTIR spectra presents some differences between the two average spectra. In of *R. globularis* sample, the signals of symmetric and asymmetric stretching from phosphates groups at 1100 cm^{-1} and 1230 cm^{-1}, conventionally assigned to the nucleic acids, are clearly visible, whereas for *R. bradyi* the signal at 1100 cm^{-1} is quite weak as the band at 1120 cm^{-1}, usually assigned to RNA. This can also be assigned to a cellular stress, as we saw for the protein material. Finally, there is also a red-shift of the main carbohydrates' peak from 1055 cm^{-1} to 1020 cm^{-1}.

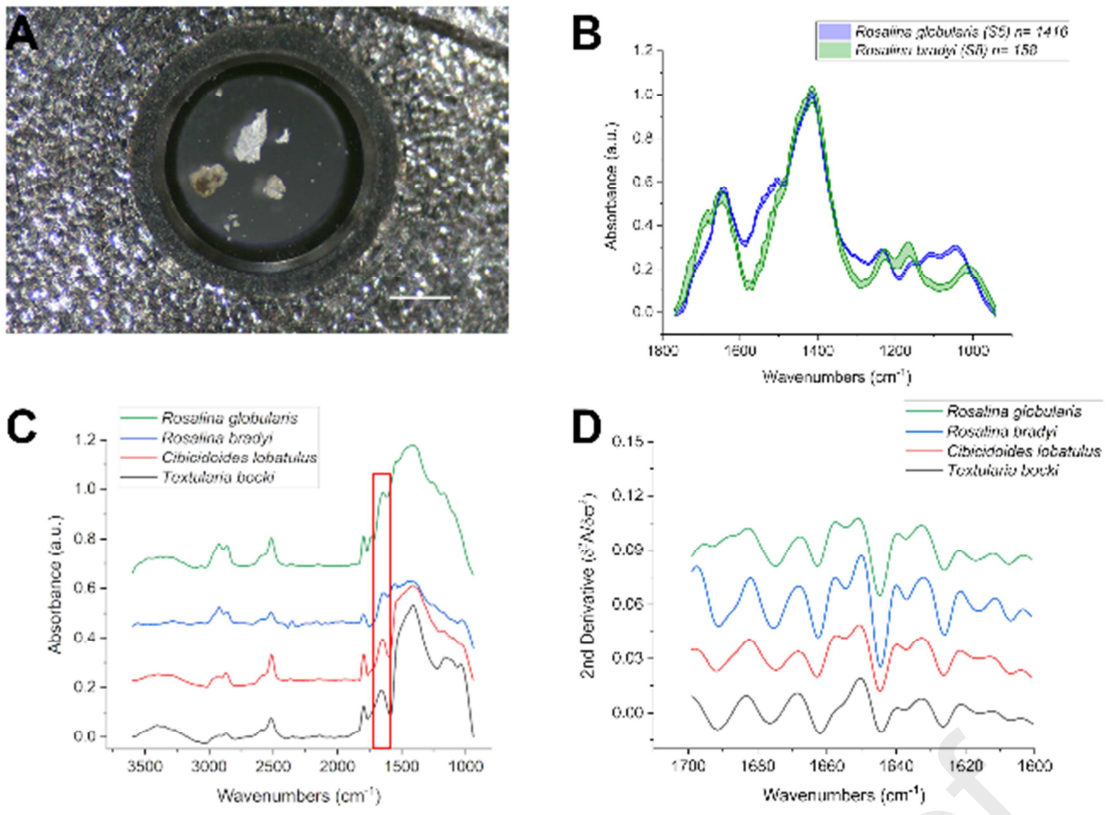

Fig. 3. A) optical image of fragments from a *R. bradyi* (S8, EPB41) inside the diamond compression cell, before being pressed. B) average spectra comparing the organic fractions of *R. bradyi* (S8 green, EPB41) and *R. globularis* (S5, negative control, blue), the line thickness corresponds to the standard deviation. C) comparison of average spectra of *T. bocki* (S1, black, EPB41), *C. lobatulus* (S3, red, EPB41), *R. bradyi* (S8, blue, EPB41), and *R. globularis* (S5 green). The grey dotted rectangle highlights the spectral range of the Amide I, that is shown in the next panel. D) second derivative of the average spectra presented in C, in the range of the Amide I, grey lines correspond to the frequencies varying the most: 1690 cm^{-1}, 1654 cm^{-1} and 1645 cm^{-1}.

In addition to *R. bradyi*, other species of foraminifera were also harvested from the Mediterranean EPB41 debris. Among these, *T. bocki* and *C. lobatulus* were considered in this study and measured in DAC in order to verify the hypothesis whether the remarks noted for *R. bradyi* are species-specific or representative to all foraminifera species. In Fig. 3C, average spectra of *T. bocki, C. lobatulus, R. bradyi* and *R. globularis* were compared. The spectra were found with peculiar absorption bands. The relative vibrational architecture seemed different for each species. Specifically, the data in Fig. 2C showed that the two *Rosalina* species present a higher content of lipids (-CH_2 signal at 3000-2800 cm^{-1}) as compared with *T. bocki* and *C. lobatulus.* In addition, we could see that the calcium carbonate signal greatly varied in intensity among the species subjected to the comparison.

Instead, considering the protein component, we could see a similar biochemical pattern than that of the samples harvested on the plastic bag. This remark is more evident in Fig. 3D, where the second derivative spectra of Amide I are shown. From this plot, it is clear that all the plastic-grown samples have a common component at 1690 cm^{-1} assigned to protein beta-sheets which is absent in the negative control-laboratory-grown samples (S5). Noticeably, intra-cellular protein aggregation into water-insoluble beta-sheets is one of the most common features suggesting pathological events displayed during oxidative-stress cytotoxicity (Krishnakumar et al., 2012; Novak et al., 2019; Shivanoor and David, 2015). The accumulation of beta aggregates within the cell is then confirmed to be a good candidate as a proxy for plastic-induced-environmental stress.

3.4. DEHP accumulation in the Rosalina globularis *cell*

The analysis set out at answering the question on whether or not DEHP accumulates in the organic fraction (i.e., the cell) of *R. globularis*. This species is routinely cultured in the laboratory and we were able to grow it in clean water (S5 specimen) and under controlled addition of net liquid DEHP (S9 specimen). In Fig. 4A, an optical image of a small fragment of *R. globularis* (S9, DEHP), deposited onto DAC, is shown. It should be emphasized that the cell was not closed to preserve the morphology of this sample in this case. Therefore, it was not possible to collect a FTIR hyperspectral image of the complete specimen that could be used to visualize the DEHP accumulation within the foraminifera, because of the thickness of the sample. Nevertheless, smaller fragments could be analyzed and the RGB map shown in Fig. 4B represents the results collected. This image was shown in RGB, the red was assigned to the DEHP band at 1730 cm^{-1}, the blue to the protein material from the cytoplasm, and the green was used to show the distribution of the calcium carbonate. From the data in Fig 4B, it can be seen that the DEHP signal is co-localized to the shell and cytoplasm.

By computing the average spectra for S5 and S9, shown in Fig. 5A, the DEHP-exposed sample (S9) was found with the highest absorbance values. Surprisingly, any strong effect of the pollutant onto the protein secondary structure could not be concluded. However, it seems possible that, the exposure to the chemical was too short to see any strong net effect and DEHP molecules are accumulated in the cellule's vacuoles and probably slightly transferred to shell carbonate material.

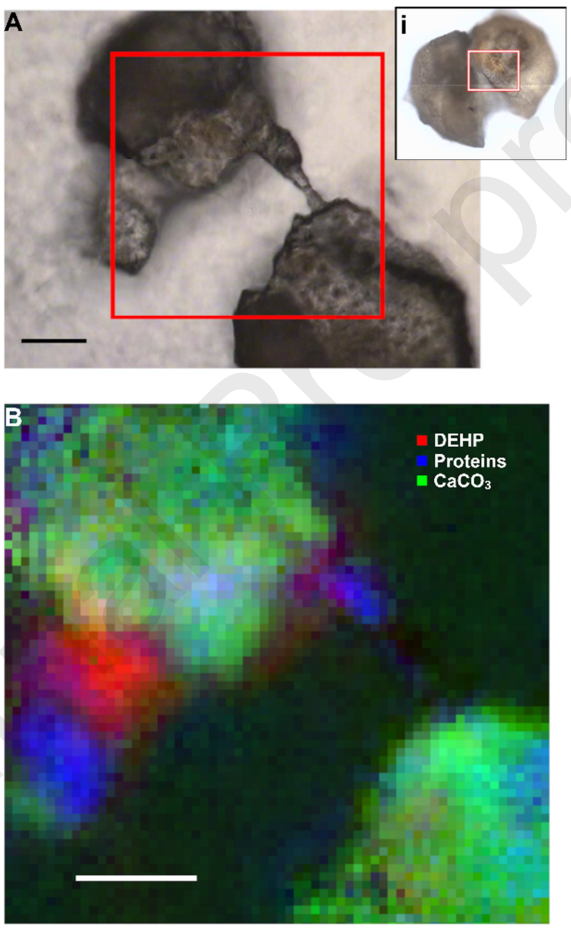

Fig. 4. A) optical image of a part of *R. globularis* (S9, DEHP) inside the diamond compression cell, after being dried. The red square is the measured area; in the inset i) Optical image of an intact *R. globularis* grew with DEHP before being dissected. B) RGB false color chemical map of the same area shown in panel A of *R. globularis* + DEHP. Scale bars: 50 microns.

To prove that DEHP accumulation yielded substantial molecular effect in the treated samples, the average spectrum of the un-treated sample was subtracted from that of the treated one. These data were shown in Fig. 5B. The net-DEHP signal was evident, as opposed to a raw DEHP spectrum. In particular, the intense DEHP bands centered at 1720 cm^{-1}, 1275 cm^{-1}, 1077 cm^{-1} as well as the whole CH-stretching range were found to be the most intense ones. Thus, we can conclude that the DEHP molecule can enter the cell of *R. globularis* and be further accumulated within the shell. To confirm further these data a second sample for the same batch was measured once the water is dried out, in Fig. 5C are shown the minimum and maximum DEHP signals measured in four different points of the sample: two inside *R. globularis* and two outside. In the specific, the points inside the cell correspond to an area comprising one pseudopodium and the cytoplasm of *R. globularis*. Instead, those outside the cell are found in small drops of DEHP that form onto the surface of the compression cell once the water, that has a lower boiling point, evaporates (see inset in Fig. 5C). It is evident from the data that the DEHP measured inside the cell is comparable or even higher than that measured outside.

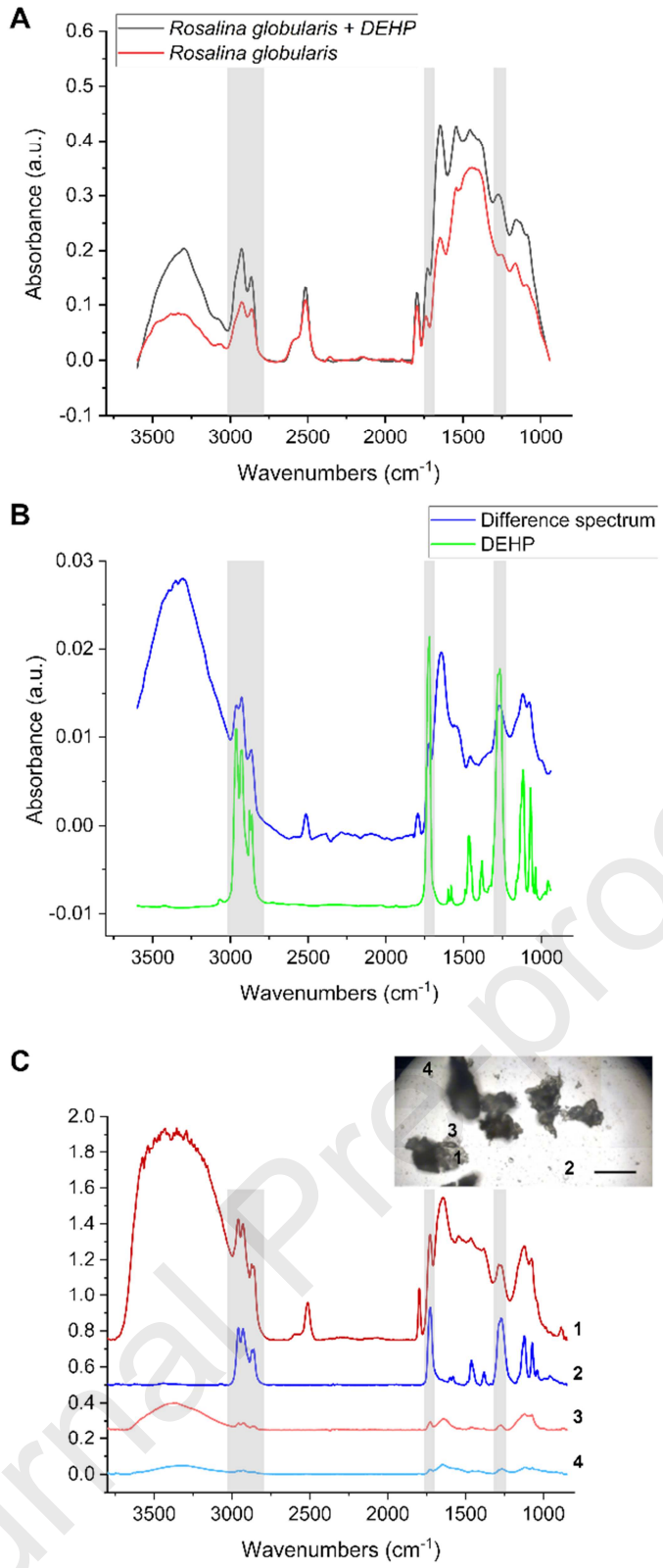

Fig. 5. A) average spectra comparing *R. globularis* (S9 black, culture with DEHP) and *R. globularis* (S5, red, culture without DEHP), B) the difference spectrum of S9 minus S5, in blue, compared to the DEHP spectrum, green line. C) four spectra representing the minima and maxima DEHP signal detectable inside S9 (tones of red) and in the surrounding area (tones of blue), after the drying of most of the water. In the inset the four locations from where the spectra were extracted. Scale bar = 200 microns.

4. Discussion

Now that microplastics have been worldwide recognized as an emerging pollutant, evaluating their effects on biota has become an urgent research priority. This is the first work, as far as we know, that investigates the impact of microplastic and their additives on foraminifera at the molecular scale. We observed a microplastics fragment, being the core around which *T. bocki* built its shell, and FTIR spectroscopy allowed to recognize the fingerprint of the epoxy resin debris. Furthermore, we found clear evidence for degradation of the polymer, which, when compared to a spectrum of a pristine epoxy resin, presents broader peaks, traces of oxidation and hydrolysis detectable by the strong C=O peak and –OH peak and local decrease of the double bonds. For this reason, the unique incorporation of plastic debris in the shell of the agglutinated species could be related to the building behavior of *T. bocki* to select and pick up these foreign elements to build its portable house. This indicates that investigated foraminifer can, at some extent, alter the plastic molecules driving plastics' biogeochemical fate.

Moreover, we individuated spectral markers providing insights on the effects that chemical stress induces on the studied foraminifera. DAC samples clearly indicate that all the samples grown on the plastic debris and *R. globularis* cultured in laboratory under acute DEHP concentrations present a signal at 1690 cm^{-1}, assigned to beta-aggregates, that is absent in *R. globularis* grown in laboratory without any stress related to plastics or DEHP.

Our results confirm the reliability of FTIR spectroscopy in discriminating between the natural and synthetic molecules and so the possibility to mark the DEHP inside the foraminiferal cytoplasm even if in other marine organisms. Several literature works (Prakash et al., 2015) report that one of the effects of micro and nano plastics presence in fishes (Alomar et al., 2017; Yu et al., 2018), marine worms (Rodríguez-Seijo et al., 2018) and even marine bacteria (Sun et al., 2018) is the production of reactive oxygen species (ROS) and the increase of the oxidative stress for the organ or whole organism. Ciacci et al. (2019) found that nanoparticles of polystyrene can be identified in cytoplasm of a foraminifer, *Ammonia parkinsoniana,* and this results in ROS and lipids production. Intra-cellular protein aggregation into water-insoluble beta-sheets is one of the most common features suggesting pathological events displayed during oxidative-stress cytotoxicity (Krishnakumar et al., 2012; Novak et al., 2019; Shivanoor and David, 2015). One of the FTIR biomarkers for oxidative stress is the increment of protein β-sheet aggregates at 1690 and 1620 cm^{-1} (Elmadany et al., 2018; González-Montalbán et al., 2007; Mitri et al., 2015; Xiong et al., 2019). Therefore, the observed accumulation of beta aggregates within the cell, often insoluble, can be used as a proxy for the suffering of the cells for different species and plastic-related-stress environmental conditions.

Literature studies monitored the short-term effect of polypropylene (PP) leachates at both environmentally realistic and chronic concentrations on the locomotion and metabolism of benthic calcareous foraminifera (Langlet et al., 2020). They found that that PP leachates have no lethal effects on this species activity. Present study shows that DEHP, even if no evidence was found for lethal effects, deeply affected cytoplasm and shell composition. In fact, our analysis of FTIR data indicated that DEHP can enter the cell of *R. globularis* and can be accumulated inside the cytoplasm. As far as we know, this is the first evidence for noticeable accumulation of DEHP in foraminiferal cytoplasm. Thus, this study opens to the possibility that DEHP enter the food web directly by unicellular organisms. Moreover, it confirms that molecular scale knowledge of cellular stress and pollutants incorporation is complementary to ecotoxicology studies.

It is worth noting that DEHP together with other phthalate esters (PAEs) has been placed on the priority pollutant list of the United States Environmental Protection Agency (U.S. EPA). DEHP is resistant to degradation, resulting in potential accumulation in aquatic communities, thus posing potential environmental threats to aquatic organisms and affecting the overall aquatic ecosystems (Zhang et al., 2018). Consequently, DEHP exposure (e.g., ingestion of food, drinking water, dust/soil, air inhalation and dermal exposure) leads to serious damage to the liver and/or reproductive system (Net et al., 2015; Notardonato et al., 2019). In our study, analysis of thin sections and DAC mounted samples indicates that *T. bocki, R. bradyi* and *C. lobatulus* grown on plastic bags, and *R. globularis* cultured under acute DEHP exposure, show lowering in organic components up to 10 times with

respect to *R. globularis* grown in pristine seawater cultures. The results from this original spectroscopic analysis indicate that plastic pollution and related molecular stress can weaken cellular processes in foraminifera.

Plastic pollution, added to ocean acidification, can have an enhanced negative effect. Particularly, in calcareous foraminiferal species target of this study, the FTIR marker related to the shell results to be weakened by plastic pollution. It is worth noting that calcareous foraminiferal shells are a biological carbon reservoir playing a moderator role in global changes and increase of partial pressure of carbon dioxide (Barker and Elderfield, 2002; Schiebel, 2002; Boyle, 1986). From this point of view, plastics dispersion in the oceans impacts on biogenic storage of carbon and, in turn, has a negative feedback leading to additional increase in the atmospheric partial pressure of carbon dioxide.

The reduced calcification together with metabolic depression were observed also for benthic foraminifera experimentally grown in polluted-artificial-seawater. Caridi et al. (2020) found that the leachate of smoked cigarette butts affects the vitality and the test building mechanism of three different benthic foraminiferal species including *R. globularis* and *T. agglutinans*. Thanks to FTIR analysis, authors supposed that the two processes: foraminiferal death and decalcification are not related but both could depend on the pH reduction measured in the cigarette butts' leachate and on the toxicity of other dissolved substances, in particular nicotine, which lead to physiology alteration and in many cases cellular death.

Conclusions.

Knowledge of molecular processes ruling pollutants incorporation in biota is an insight into the assessment of the overall impact of pollutants on the oceans. As far as we know, this is the first molecular scale study that aims at determining the effects that plastics and related chemical residues (DEHP) have on foraminifera health status and biomineralization process. To recognize the presence of microplastics debris and DEHP in the cytoplasm and the shell of this set of samples and to probe the status of the biological material, FTIR (Fourier Transform Infrared) microscopy was used. FTIR data allowed to answer the question whether there are any noticeable biochemical differences in the shells and the cytoplasm depending on the exposure of the cell organism to microplastics and bio-accessible plasticizers. The analysis of FTIR measurements consisting of thousands of spectra collected on 22 different samples show that: 1) microplastics debris can be found in the cytoplasm and inside the agglutinated test of *T. bocki*; 2) *C. lobatulus, R. bradyi* and *T. bocki*, grown on plastic remains, show signals of oxidative stress and protein aggregation; 3) DEHP can be incorporated in the cytoplasm of the commonly calcareous foraminifera *R. globularis,* thus entering biogeochemical cycles.

Polymers belonging to cellular machinery can be found both in the cytoplasm (rich in proteins, lipids, polysaccharides) and in the shell which is commonly made of calcite with different Mg concentration (calcareous tests such as *C. lobatulus, R. bradyi* and *R. globularis*), also containing natural biopolymers or formed by sediment particles glued together with a variety of cements (agglutinated tests such as *T. bocki*). This underlies high propensity of synthetic polymeric molecules for incorporation to foraminifera. The accumulation of beta aggregates within the cell is then confirmed to be a good candidate as a proxy for plastic-induced-environmental stress.

This work demonstrated that foraminifera are good proxy of on-going plastic pollution and if the associated molecules can be found in their shell, they can be candidate to detect the history of the plastic pollution in future investigations over several past decades because foraminifera are able to fossilize. Plastics undergo through biogeochemical cycling not only because the comminution due to biological activity, but also because of biochemical processes can enhance or induce some oxidation of plastics molecules. Our findings proved that microscopic FTIR analysis is an effective tool to investigate molecular-scale processes of interaction among plastics and foraminifera cytoplasm and shell. The possibility of analyzing spectral maps and specific spectral features was particularly useful to assess and compare the status of shells and cells. Future work will be addressed to characterize at the molecular scale the biogeochemical cycle of plastics considering other pollutant molecules and

foraminifera species. Plastic pollutions and ocean acidification can have together a cumulative effect potentially affecting the foraminifera biogenic storage capacity before the 2100 forecast of Uthicke et al. (2013).

Acknowledgments.
FTIR measurements were conducted in the framework of CERIC 20177040 “Incorporation of pollutants in foraminiferal shells: tools for biomonitoring” and 20192072 CERIC “Fate of metals and pollutants in marine benthic micro- and macrofauna”. The authors wish to acknowledge the captains and crews of R/V Minerva for their assistance in the collection of data. GDG wish to acknowledge TESTARE grant (Sardegna Ricerche grant number F21B17000790005). CM acknowledges the grant Excellence Departments, MIUR (ARTICOLO 1, COMMI 314 –337 LEGGE 232/2016). In this work, FC and AS cultured foraminifera in AQ University laboratory and provided foraminifera to CB and DM that cultured foraminifera in CAG University. LDB and MP provided EPB41 samples. MAC provided microtome cuts. AS, GB and LV conducted FTIR data collection and analysis. GDG, CM and DM coordinated CERIC-ERIC research activities. All the authors equally contributed to the experiment conception and writing the paper.

References

Alomar, C., Sureda, A., Capó, X., Guijarro, B., Tejada, S., Deudero, S., 2017. Microplastic ingestion by *Mullus surmuletus* Linnaeus, 1758 fish and its potential for causing oxidative stress. Environ. Res. 159, 135–142. https://doi.org/10.1016/j.envres.2017.07.043

Alve, E., Lepland, A., Magnusson, J., Backer-Owe, K., 2009. Monitoring strategies for re-establishment of ecological reference conditions: Possibilities and limitations. Mar. Pollut. Bull. 59, 297–310. https://doi.org/10.1016/j.marpolbul.2009.08.011

Armynot du Châtelet, E., Debenay, J.P., 2010. The anthropogenic impact on the western French coasts as revealed by foraminifera: A review. Rev. Micropaleontol. 53, 129–137. https://doi.org/10.1016/j.revmic.2009.11.002

Auta, H.S., Emenike, C.U., Fauziah, S.H., 2017. Distribution and importance of microplastics in the marine environment: A review of the sources, fate, effects, and potential solutions. Environ. Int. 102, 165–176. https://doi.org/10.1016/j.envint.2017.02.013

Barker, S., Elderfield, H., 2002. Foraminiferal Calcification Response to Glacial-Interglacial Changes in Atmospheric CO_2. Science 297, 833–836. Doi: 10.1126/science.1072815

Barras, C., Jorissen, F.J., Labrune, C., Andral, B., Boissery, P., 2014. Live benthic foraminiferal faunas from the French Mediterranean Coast: Towards a new biotic index of environmental quality. Ecol. Indic. 36, 719–743. https://doi.org/10.1016/j.ecolind.2013.09.028

Barth, A., 2007. Infrared spectroscopy of proteins. Biochim. Biophys. Acta-Bioenerg. 1767, 1073–1101. https://doi.org/10.1016/j.bbabio.2007.06.004

Baztan, J., Bergmann, M., Carrasco, A., Fossi, M., Jorgensen, B., Miguelez, A., Pahl, S., Thompson, R., Vanderlinden, J.-P., 2018. MICRO 2018. Fate and Impact of Microplastics: Knowledge, Actions and Solutions. Conference Proceedings Book. e-isbn: 978-84-09-06477-9

Bouchet, V.M.P., Deldicq, N., Baux, N., Dauvin, J.-C., Pezy, J.-P., Seuront, L., Méar, Y., 2020. Benthic foraminifera to assess ecological quality statuses: The case of salmon fish farming. Ecol. Indic. 117, 106607. https://doi.org/10.1016/j.ecolind.2020.106607

Bouchet, V.M.P., Goberville, E., Frontalini, F., 2018. Benthic foraminifera to assess Ecological Quality Statuses in Italian transitional waters. Ecol. Indic. 84, 130–139. https://doi.org/10.1016/j.ecolind.2017.07.055

Boyle, E.A., 1986. Paired carbon isotope and cadmium data from benthic foraminifera: Implications for changes in oceanic phosphorus, oceanic circulation, and atmospheric carbon dioxide. Geochim. Cosmochim. Acta 50, 265–276. https://doi.org/10.1016/0016-7037(86)90175-4

Boyle, E.A., Keigwin, L.D., 1985. Comparison of Atlantic and Pacific paleochemical records for the last 215,000 years: changes in deep ocean circulation and chemical inventories. Earth Planet. Sci. Lett. 76, 135–150. https://doi.org/10.1016/0012-821X(85)90154-2

Caridi, F., Sabbatini, A., Birarda, G., Costanzi, E., De Giudici, G., Galeazzi, R., Medas, D., Mobbili, G., Ricciutelli, M., Ruello, M.L., Vaccari, L., Negri, A., 2020. Cigarette butts, a threat for marine environments: Lessons from benthic foraminifera (Protista). Mar. Environ. Res. 162, 105150. https://doi.org/10.1016/j.marenvres.2020.105150

Casalbore, D., Ridente, D., Bosman, A., Chiocci, F.L., 2017. Depositional and erosional bedforms in Late Pleistocene-Holocene pro-delta deposits of the Gulf of Patti (southern Tyrrhenian margin, Italy). Mar. Geol. 385, 216–227. https://doi.org/10.1016/j.margeo.2017.01.007

Cau, A., Avio, C.G., Dessì, C., Moccia, D., Pusceddu, A., Regoli, F., Cannas, R., Follesa, M.C., 2020. Benthic Crustacean Digestion Can Modulate the Environmental Fate of Microplastics in the Deep Sea. Environ. Sci. Technol. 54, 4886–4892. https://doi.org/10.1021/acs.est.9b07705

Celia Magno, M., Bergamin, L., Finoia, M.G., Pierfranceschi, G., Venti, F., Romano, E., 2012. Correlation between textural characteristics of marine sediments and benthic foraminifera in highly anthropogenically-altered coastal areas. Mar. Geol. 315-318, 143–161. https://doi.org/10.1016/j.margeo.2012.04.002

Ciacci, C., Grimmelpont, M.V., Corsi, I., Bergami, E., Curzi, D., Burini, D., Bouchet, V.M.P., Ambrogini, P., Gobbi, P., Ujiié; Y., Ishitani, Y., Coccioni, R., Bernhard, J.M., Frontalini, F., 2019. Nanoparticle-biological interactions in a marine benthic foraminifer. Sci. Rep. 9, 19441. https://doi.org/10.1038/s41598-019-56037-2

Cimerman, F., Langer, M.R., 1991. Mediterranean foraminifera. Accademia Scientiarum et Artium Slovenica, Ljubljana.

Curry, W.B., Duplessy, J.C., Labeyrie, L.D., Shackleton, N.J., 1988. Changes in the distribution of δ13C of deep water ΣCO_2 between the Last Glaciation and the Holocene. Paleoceanography 3, 317–341. https://doi.org/10.1029/PA003i003p00317

Damak, M., Fourati, R., Ellech, B., Kallel, M., 2019. Assessment of organic and metallic contamination in the surface sediment of Monastir Bay (Eastern Tunisia): Spatial distribution, potential sources, and ecological risk assessment. Mar. Pollut. Bull. 149, 110500. https://doi.org/10.1016/j.marpolbul.2019.110500

de Sá, L.C., Oliveira, M., Ribeiro, F., Rocha, T.L., Futter, M.N., 2018. Studies of the effects of microplastics on aquatic organisms: What do we know and where should we focus our efforts in the future? Sci. Total Environ. 645, 1029–1039. https://doi.org/10.1016/j.scitotenv.2018.07.207

Doherty, J., Cinque, G., Gardner, P., 2017. Single-cell analysis sing Fourier transform infrared microspectroscopy, Appl. Spectrosc. Rev. 52, 560–587. https://doi.org/10.1080/05704928.2016.1250214

Dolven, J.K., Alve, E., Rygg, B., Magnusson, J., 2013. Defining past ecological status and in situ reference conditions using benthic foraminifera: A case study from the Oslofjord, Norway. Ecol. Indic. 29, 219–233. https://doi.org/10.1016/j.ecolind.2012.12.031

Elmadany, N., Khalil, E., Vaccari, L., Birarda, G., Yousef, I., Abu-Dahab, R., 2018. Antiproliferative activity of the combination of doxorubicin/quercetin on MCF7 breast cancer cell line: A combined study using colorimetric assay and synchrotron infrared microspectroscopy. Infrared Phys. Technol. 95, 141–147. https://doi.org/10.1016/j.infrared.2018.10.014

Enders, K., Käppler, A., Biniasch, O., Feldens, P., Stollberg, N.r. Lange, X., Fischer, D., Eichhorn, K.-J., Pollehne, F., Oberbeckmann, S., Labrenz, M., 2019. Tracing microplastics in aquatic environments based on sediment analogies. Sci. Rep. 9, 15207. https://www.nature.com/articles/s41598-019-50508-2

Fossi, M.C., Panti, C., Guerranti, C., Coppola, D., Giannetti, M., Marsili, L., Minutoli, R., 2012. Are baleen whales exposed to the threat of microplastics? A case study of the Mediterranean fin whale (*Balaenoptera physalus*). Mar. Pollut. Bull. 64, 2374–2379. https://doi.org/10.1016/j.marpolbul.2012.08.013

Fossile, E., Sabbatini, A., Spagnoli, F., Dell'Anno, A., de Marco, R., Dinelli, E., Droghini, E., Tramontana, M., Negri, A., 2021. Sensitivity of foraminiferal-based indices to evaluate the ecological quality status of marine coastal benthic systems: a case study of the Gulf of Manfredonia (Southern Adriatic Sea). Mar. Pollut. Bull. 163, 111933. https://doi.org/10.1016/j.marpolbul.2020.111933

Frontalini, F., Curzi, D., Giordano, F.M., Bernhard, J.M., Falcieri, E., Coccioni, R., 2015. Effects of lead pollution on *Ammonia parkinsoniana* (foraminifera): ultrastructural and microanalytical approaches. Eur. J. Histochem. 59, 2460. Doi: 10.4081/ejh.2015.2460

Geyer, R., Jambeck, J.R., Law, K.L., 2017. Production, use, and fate of all plastics ever made. Sci. Adv. 3, e1700782. Doi: 10.1126/sciadv.1700782

Gibbons, J.A., Alexander, M., 1989. Microbial degradation of sparingly soluble organic chemicals: Phthalate esters. Environ. Toxicol. Chem. 8, 283–291. https://doi.org/10.1002/etc.5620080404

González-Montalbán, N., Villaverde, A., Aris, A., 2007. Amyloid-linked cellular toxicity triggered by bacterial inclusion bodies. Biochem. Biophys. Res. Commun. 355, 637–642. https://doi.org/10.1016/j.bbrc.2007.01.192

Graham, P.R., 1973. Phthalate ester plasticizers-why and how they are used. Environ. Health Perspect. 3, 3–12. Doi:10.1289/ehp.73033

Grefstad, A.I., 2019. Marine benthic foraminifera and microplastics (Accumulation and effects following short- and long-term exposure). Master thesis, Faculty of Mathematics and Natural Sciences, Department of Biosciences Universitetet I Oslo. http://urn.nb.no/URN:NBN:no-75117

Harris, C.R., Millman, K.J., van der Walt, S.J., Gommers, R., Virtanen, P., Cournapeau, D., Wieser, E., Taylor, J., Berg, S., Smith, N.J., Kern, R., Picus, M., Hoyer, S., van Kerkwijk, M.H., Brett, M., Haldane, A., del Río, J.F., Wiebe, M., Peterson, P., Gérard-Marchant, P., Sheppard, K., Reddy, T., Weckesser, W., Abbasi, H., Gohlke, C., Oliphant, T.E., 2020. Nature 585, 357–362. https://doi.org/10.1038/s41586-020-2649-2

Hoang, V.L.T., Li, Y., Kim, S.K., 2008. Cathepsin B inhibitory activities of phthalates isolated from a marine Pseudomonas strain. Bioorg. Med. Chem. Lett. 18, 2083–2088. https://doi.org/10.1016/j.bmcl.2008.01.097

Holman, H.□Y.N., Martin, M.C., Blakely, E.A., Bjornstad, K., Mckinney, W.R., 2000. IR spectroscopic characteristics of cell cycle and cell death probed by synchrotron radiation based Fourier transform IR spectromicroscopy. Biopolymers 57, 329–335. https://doi.org/10.1002/1097-0282(2000)57:6<329::AID-BIP20>3.0.CO;2-2

Hunter, J.D., 2007. Matplotlib: A 2D Graphics Environment. Comput. Sci. Eng. 9, 90–95. Doi: 10.1109/MCSE.2007.55

Jambeck, J.R., Geyer, R., Wilcox, C., Siegler, T.R., Perryman, M., Andrady, A., Narayan, R., Law, K.L., 2015. Plastic waste inputs from land into the ocean. Science 347, 768–771. Doi: 10.1126/science.1260352

Jamin, N., Dumas, P., Moncuit, J., Fridman, W.H., Teillaud, J.L., Carr, G.L., Williams, G.P., 1998. Chemical imaging of nucleic acids, proteins and lipids of a single living cell. Application of synchrotron infrared microspectrometry in cell biology. Cell. Mol. Biol. 44, 9–13.

Kawahata, H., Fujita, K., Iguchi, A., Inoue, M., Iwasaki, S., Kuroyanagi, A., Maeda, A., Manaka, T., Moriya, K., Takagi, H., Toyofuku, T., Yoshimura, T., Suzuki, A., 2019. Perspective on the response of marine calcifiers to global warming and ocean acidification—Behavior of corals and foraminifera in a high CO_2 world "hot house". Prog. Earth Planet. Sci. 6, 5. https://doi.org/10.1186/s40645-018-0239-9

Kellner, R., Fischböck, G., Minich, C., 1986. FTIR-microscopy versus FTIR-ATR-spectroscopy for the analysis of multilayer polymer films. Mikrochim. Acta 88, 271–279. https://doi.org/10.1007/BF01206720

Kellner, R., Weigel, C., 1988. Pushing the limits of quantitative FTIR-microscopy. Mikrochim. Acta 94, 163–166. https://doi.org/10.1007/BF01205861

Koo, H.J., Lee, B., 2004. Estimated exposure to phthalates in cosmetics and risk assessment. J. Toxicol. Environ. Health A 67, 1901–14. https://doi.org/10.1080/15287390490513300

Krishnakumar, N., Prabu, S.M., Sulfikkarali, N.K., 2012. Quercetin protects against cadmium-induced biochemical and structural changes in rat liver revealed by FT-IR spectroscopy. Biomed. Prev. Nutr. 2, 179–185. https://doi.org/10.1016/j.bionut.2012.03.010

Langer, M.R., 2008. Assessing the contribution of foraminiferan protists to global ocean carbonate production. J. Eukaryot. Microbiol. 55, 163–169. https://doi.org/10.1111/j.1550-7408.2008.00321.x

Langlet, D., Bouchet, V.M.P., Delaeter, C., Seuront, L., 2020. Motion behavior and metabolic response to microplastic leachates in the benthic foraminifera *Haynesina germanica*. J. Exp. Mar. Biol. Ecol. 529, 151395. https://doi.org/10.1016/j.jembe.2020.151395

Legal, J.M., Manfait, M., Theophanides, T., 1991. Applications of FTIR spectroscopy in structural studies of cells and bacteria. J. Mol. Struct. 242, 397–407. https://doi.org/10.1016/0022-2860(91)87150-G

Ljungvall, K., Veeramachaneni, D.N.R., Hou, M., Hultén, F., Magnusson, U., 2008. Morphology and morphometry of the reproductive organs in prepubertal and postpubertal male pigs exposed to di(2-ethylhexyl) phthalate before puberty: Precocious development of bulbourethral glands. Theriogenology 70, 984–991. https://doi.org/10.1016/j.theriogenology.2008.05.061

Luo, Q., Liu, Z.-h., Yin, H., Dang, Z., Wu, P.-x., Zhu, N.-w., Lin, Z., Liu, Y., 2018. Migration and potential risk of trace phthalates in bottled water: A global situation. Water Res. 147, 362–372. https://doi.org/10.1016/j.watres.2018.10.002

Mitri, E., Kenig, S., Coceano, G., Bedolla, D.E., Tormen, M., Grenci, G., Vaccari, L., 2015. Time-Resolved FT-IR Microspectroscopy of Protein Aggregation Induced by Heat-Shock in Live Cells. Anal. Chem. 87, 3670–3677. https://doi.org/10.1021/ac5040659

Movasaghi, Z., Rehman, S., Rehman, I.U., 2008. Fourier Transform Infrared (FTIR) Spectroscopy of biological tissues. Appl. Spectrosc. Rev. 43, 134–179. https://doi.org/10.1080/05704920701829043

Murray, J.W., 2006. Ecology and Applications of Benthic Foraminifera. Cambridge University Press, New York.

Net, S., Sempéré, R., Delmont, A., Paluselli, A., Ouddane, B., 2015. Occurrence, fate, behavior and ecotoxicological state of phthalates in different environmental matrices. Environ. Sci. Technol. 49, 4019−4035. https://doi.org/10.1021/es505233b

Notardonato, I., Protano, C., Vitali, M., Bhattacharya, B., Avino, P., 2019. A method validation for simultaneous determination of phthalates and bisphenol a released from plastic water containers. Appl. Sci. 9, 2945. https://doi.org/10.3390/app9142945

Novak, S., Romih, T., Drašler, B., Birarda, G., Vaccari, L., Ferraris, P., Sorieul, S., Zieba, M., Sebastian, V., Arruebo, M., Hočevar, S.B., Jemec Kokalj, A., Drobne, D., 2019. The in vivo effects of silver nanoparticles on terrestrial isopods, *Porcellio scaber*, depend on a dynamic interplay between shape, size and nanoparticle dissolution properties. Analyst 144, 488–497. https://doi.org/10.1039/C8AN01387J

Parsaian, M., Shokri, M.R., Pazooki, J., 2018. The response of benthic foraminifera to aquaculture and industrial pollution: A case study from the Northern Persian Gulf. Mar. Pollut. Bull. 135, 682–693. https://doi.org/10.1016/j.marpolbul.2018.07.073

Pazos, R.S., Bauer, D.E., Gómez, N., 2018. Microplastics integrating the coastal planktonic community in the inner zone of the Río de la Plata estuary (South America). Environ. Pollut. 243, 134–142. ttps://doi.org/10.1016/j.envpol.2018.08.064

Peeken, I., Primpke, S., Beyer, B., Gütermann, J., Katlein, C., Krumpen, T., Bergmann, M., Hehemann, L., Gerdts, G., 2018. Arctic sea ice is an important temporal sink and means of transport for microplastic. Nat. Commun. 9, 1505. https://doi.org/10.1038/s41467-018-03825-5

Picó, Y., Barceló, D., 2019. Analysis and prevention of microplastics pollution in water: current perspectives and future directions. ACS Omega 4, 6709–6719. https://doi.org/10.1021/acsomega.9b00222

Prakash, C., Kamboj, V.K., Ahlawat, P., Kumar, V., 2015. Structural and molecular alterations in arsenic-induced hepatic oxidative stress in rats: a FTIR study. Toxicol. Environ. Chem. 97, 408–1421. https://doi.org/10.1080/02772248.2015.1102425

Redondo-Hasselerharm, P.E., Falahudin, D., Peeters, E.T.H.M., Koelmans, A.A., 2018. Microplastic effect thresholds for freshwater benthic macroinvertebrates. Environ. Sci. Technol. 52, 2278–2286. https://doi.org/10.1021/acs.est.7b05367

Rodríguez-Seijo, A., da Costa, J.P., Rocha-Santos, T., Duarte, A.C., Pereira, R., 2018. Oxidative stress, energy metabolism and molecular responses of earthworms (*Eisenia fetida*) exposed to low-density polyethylene microplastics. Environ. Sci. Pollut. Res. 25, 33599–33610. https://doi.org/10.1007/s11356-018-3317-z

Roy, R.N., Laskar, S., Sen, S.K., 2006. Dibutyl phthalate, the bioactive compound produced by *Streptomyces albidoflavus* 321.2. Microbiol. Res. 161, 121–126. https://doi.org/10.1016/j.micres.2005.06.007

Sanna, R., Medas, D., Podda, F., Meneghini, C., Casu, M., Lattanzi, P., Scorciapino, M.A., Floris, C., Cannas, C., De Giudici, G., 2015. Binding of bis-(2-ethylhexyl) phthalate at the surface of hydrozincite nanocrystals: An example of organic molecules absorption onto nanocrystalline minerals. J. Colloid Interface Sci. 457, 298–306. https://doi.org/10.1016/j.jcis.2015.07.016

Schiebel, R., 2002. Planktic foraminiferal sedimentation and the marine calcite budget. Glob. Biogeochem. Cycles, 16, 1065. https://doi.org/10.1029/2001GB001459

Sen Gupta, B.K., 1999. Modern Foraminifera. Kluwer Academic Publishers, Great Britain.

Sgarrella, F., Moncharmont Zei, M., 1993. Benthic foraminifera of the Gulf of Naples (Italy): systematics and autoecology. Boll. Soc. Paleontol. Ital. 32, 145–264.

Shim, W.J., Thomposon, R.C., 2015. Microplastics in the Ocean. Arch. Environ. Contam. Toxicol. 69, 265–268. https://doi.org/10.1007/s00244-015-0216-x

Shivanoor, S.M., David, M., 2015. Fourier transform infrared (FT-IR) study on cyanide induced biochemical and structural changes in rat sperm. Toxicol. Rep. 2, 1347–1356. https://doi.org/10.1016/j.toxrep.2015.10.004

Silverstein, R.M., Webster, F.X., Kiemle, D.J., 2005. Spectrometric identification of organic compounds. John Wiley & Sons, Hoboken, NJ.

Singh, S., Sinha, R., Häder, D., 2002. Role of lipids and fatty acids in stress tolerance in Cyanobacteria. Acta protozool. 41, 297–308.

Stanley, M.K., Robillard, K.A., Staples, C.A., 2003. Introduction, in: Staples, C.A. (Eds.), Phthalate Esters. Springer-Verlag, Berlin, pp. 1–7.

Sun, X., Chen, B., Li, Q., Liu, N., Xia, B., Zhu, L., Qu, K., 2018. Toxicities of polystyrene nano- and microplastics toward marine bacterium *Halomonas alkaliphila*. Sci. Total Environ. 642, 1378–1385. https://doi.org/10.1016/j.scitotenv.2018.06.141

Uthicke, S., Momigliano, P., Fabricius, K., 2013. High risk of extinction of benthic foraminifera in this century due to ocean acidification. Sci. Rep. 3, 1769. https://doi.org/10.1038/srep01769

Vandermeersch, G., Van Cauwenberghe, L., Janssen, C.R., Marques, A., Granby, K., Fait, G., Kotterman, M.J.J., Diogène, J., Bekaert, K., Robbens, J., Devriese, L., 2015. A critical view on microplastic quantification in aquatic organisms. Environ. Res. 143, 46–55. https://doi.org/10.1016/j.envres.2015.07.016

Vénec-Peyré, M.T., Bartolini, A., Weber, M., Lipps, J.H., 2020. Morphological deformation of foraminiferal tests caused by intertidal oil sills (Black Tides), in: Guex, J., Torday J.S., Miller Jr. W. (Eds.), Morphogenesis, Environmental Stress and Reverse Evolution. Springer, Cham., pp. 175–196. https://doi.org/10.1007/978-3-030-47279-5_9

Wetzel, D.L., LeVine, S.M., 1999. Imaging molecular chemistry with infrared microscopy. Science 285, 1224–1225. Doi: 10.1126/science.285.5431.1224

Wiley John & Sons, Inc., 2020. SpectraBase; **https://spectrabase.com/** (accessed 12/12/2020).

WoRMS (2020). Foraminifera. Accessed at: http://www.marinespecies.org/aphia.php?p=taxdetails&id=1410 on 2020-11-11

Xiong, Q., Hu, L.-X., Liu, Y.-S., Wang, T.-T., Ying, G.-G., 2019. New insight into the toxic effects of chloramphenicol and roxithromycin to algae using FTIR spectroscopy. Aquat. Toxicol. 207, 197–207. https://doi.org/10.1016/j.aquatox.2018.12.017

Yu, P., Liu, Z., Wu, D., Chen, M., Lv, W., Zhao, Y., 2018. Accumulation of polystyrene microplastics in juvenile *Eriocheir sinensis* and oxidative stress effects in the liver. Aquat. Toxicol. 200, 28–36. https://doi.org/10.1016/j.aquatox.2018.04.015

Zhang, Z.-M., Zhang, H.-H., Zhang, J., Wang, Q.-W., Yang, G.-P., 2018. Occurrence, distribution, and ecological risks of phthalate esters in the seawater and sediment of Changjiang River Estuary and its adjacent area. Sci. Total Environ. 619–620, 93–102. https://doi.org/10.1016/j.scitotenv.2017.11.070

- Foraminifera can use plastic debris to build agglutinated tests
- Plastic debris in foraminifera can undergo oxidation
- Phthalate molecule can enter the body of foraminifera
- Plastic can affect foraminiferal cellules
- Ocean acidification and plastic pollution can have a cumulative effect

Declaration of interests

☒ The authors declare that they have no known competing financial interests or personal relationships that could have appeared to influence the work reported in this paper.

☐The authors declare the following financial interests/personal relationships which may be considered as potential competing interests: